Supporting Information

Uracil-5-yl *O*-Sulfamate: An Illusive Radiosensitizer. Pitfalls in Modeling the Radiosensitizing Derivatives of Nucleobases

Paulina Spisz,[1] Magdalena Zdrowowicz,[1] Witold Kozak,[1] Lidia Chomicz-Mańka,[1] Karina Falkiewicz,[1] Samanta Makurat,[1] Artur Sikorski,[1] Dariusz Wyrzykowski,[1] Janusz Rak,[1*] Eugene Arthur-Baidoo[4], Patrick Ziegler,[4] Mateus Salomao Rodrigues Costa,[4] and Stephan Denifl[4*]

[1] Group of Biological Sensitizers, Physical Chemistry Department, Faculty of Chemistry, University of Gdańsk, 80-308 Gdańsk, Poland

[2] Group of Crystallochemistry, Physical Chemistry Department, Faculty of Chemistry, University of Gdańsk, 80-308 Gdańsk, Poland

[3] Group of Physicochemistry and Complex Compounds, General and Inorganic Chemistry Department, Faculty of Chemistry, University of Gdańsk, 80-308 Gdańsk, Poland

[4] Institut für Ionenphysik und Angewandte Physik and Center for Biomolecular Sciences Innsbruck, Leopold-Franzens Universität Innsbruck, Technikerstrasse 25, A-6020 Innsbruck, Austria

*To whom correspondence should be addressed.

Table S1. Crystal data and structure refinement parameters for uracil-5-yl *O*-sulfamate.

Compound	uracil-5-yl *O*-sulfamate
Chemical formula	$C_4H_5N_3O_5S$
FW/g·mol^{-1}	207.17
Crystal system	Monoclinic
Space group	$P2_1/n$
a/Å	4.873(3)
b/Å	9.071(5)
c/Å	16.547(9)
α/°	90
β/°	97.07(3)
γ/°	90
V/Å^3	725.9(2)
Z	4
T/K	295(2)
λ_{Mo}/Å	0.71073
ρ_{calc}/g·cm^{-3}	1.896
F(000)	424
μ/mm^{-1}	0.442
θ range/°	3.35–25.00
Completeness θ/%	99.9
Reflections collected	4358
Reflections unique	1281 [R_{int} = 0.1061]
Data/restraints/parameters	1281/0/130
Goodness of fit on F^2	0.972
Final R_1 value ($I>2\sigma(I)$)	0.0610
Final wR_2 value ($I>2\sigma(I)$)	0.0865
Final R_1 value (all data)	0.1106
Final wR_2 value (all data)	0.1572
CCDC number	1997918

Table S2. Hydrogen bonding interactions in the crystal structure of title compound.

D–H···A	*d*(D–H) (Å)	*d*(H···A) (Å)	*d*(D···A) (Å)	<D–H···A (°)
N1–H1···O7^{i}	0.90(5)	1.92(5)	2.795(6)	163(5)
N3–H3···O8^{ii}	0.73(6)	2.16(6)	2.887(7)	173(6)
N13–H13A···O8^{iii}	0.85(6)	2.11(6)	2.941(7)	167(6)
N13–H13B···O12^{iv}	1.00(5)	1.98(5)	2.951(7)	164(4)
C6–H6···O12^{iii}	0.93	2.44	3.318(8)	157

Symmetry codes: (i) −1−x,1−y,2−z; (ii) −x,2−y,2−z; (iii) 1/2−x, −1/2+y,3/2−z; (iv) −1+x,y,z.

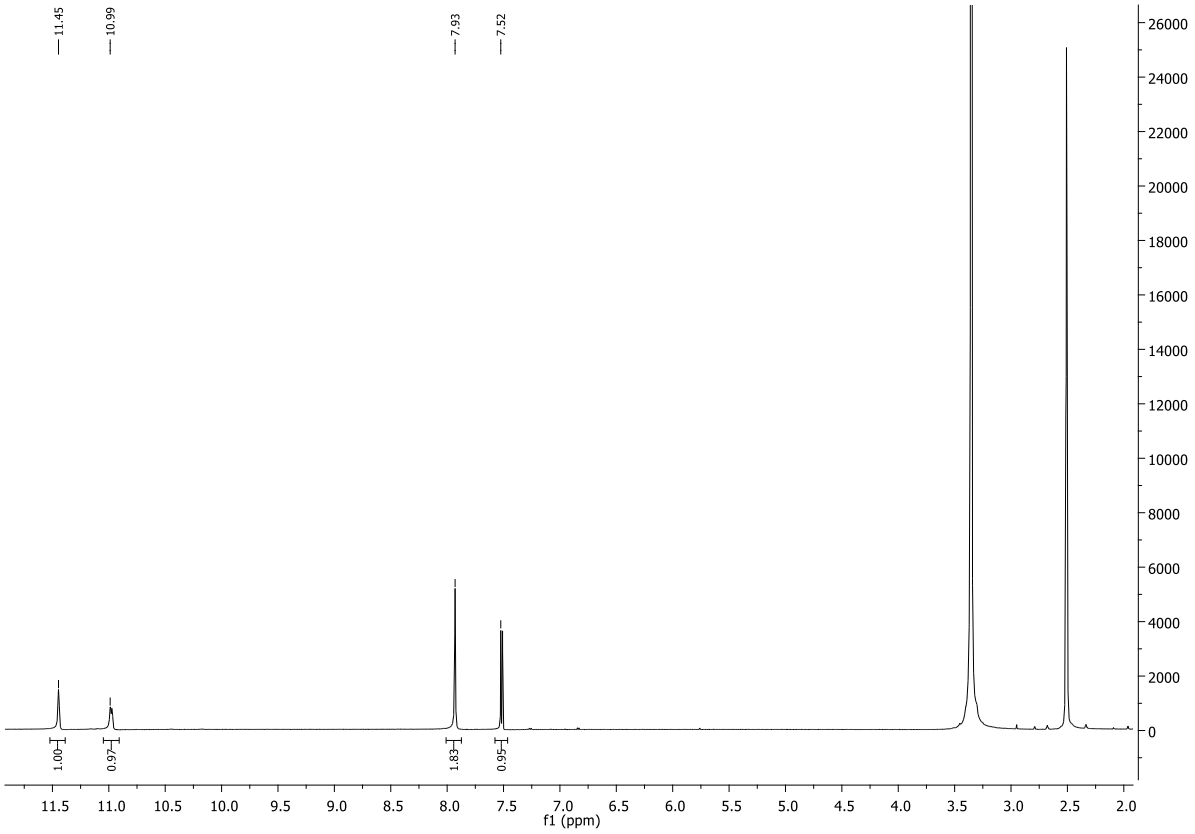

Figure S1. ^{1}H NMR spectrum of uracil-5-yl *O*-sulfamate.

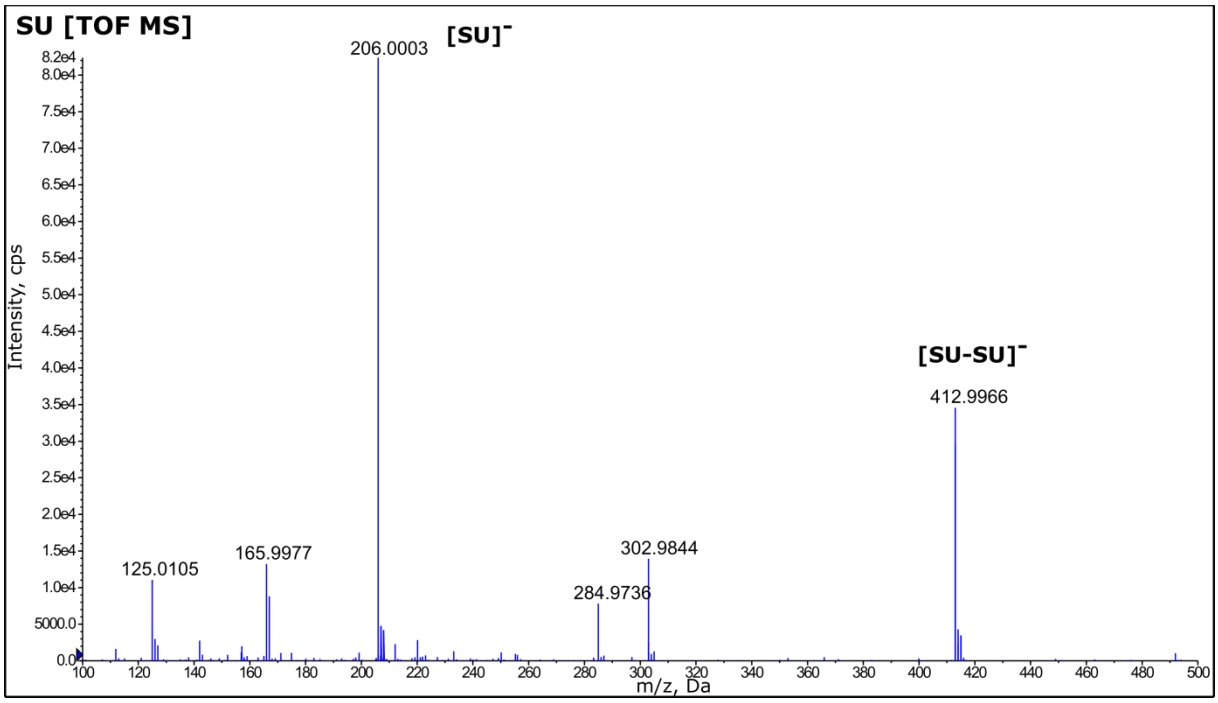

Figure S2. MS spectrum (in negative mode) of uracil-5-yl *O*-sulfamate.

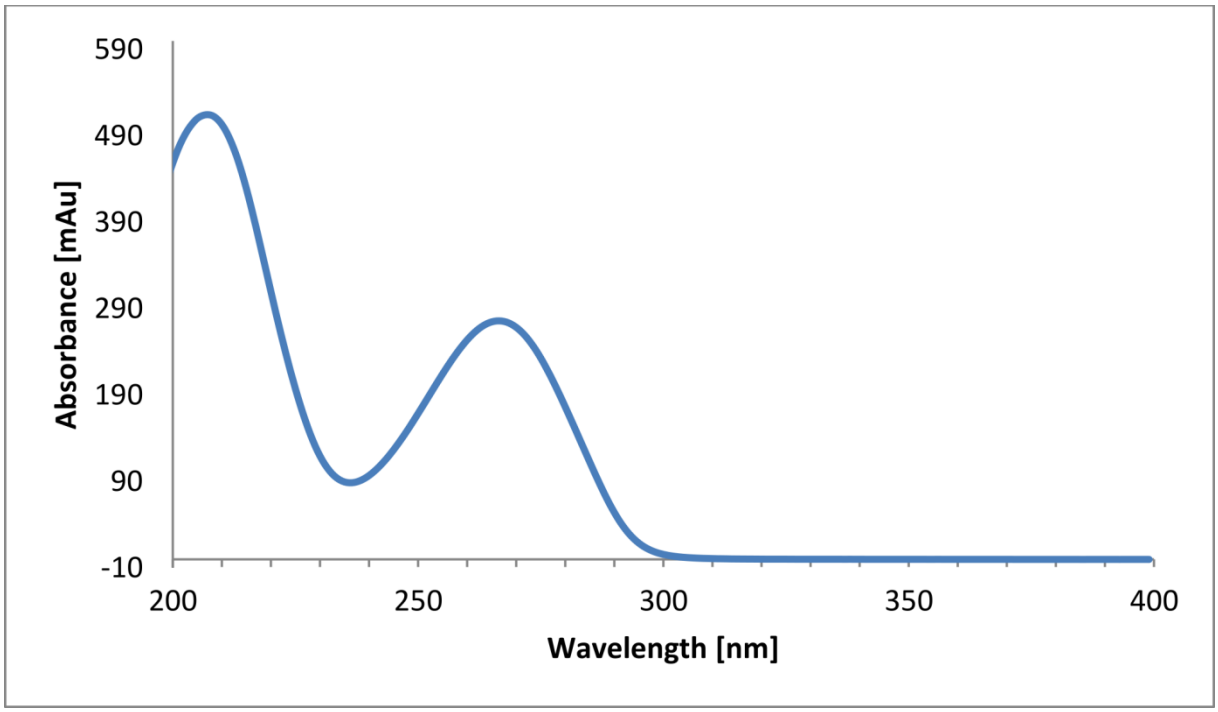

Figure S3. UV spectrum of uracil-5-yl *O*-sulfamate.

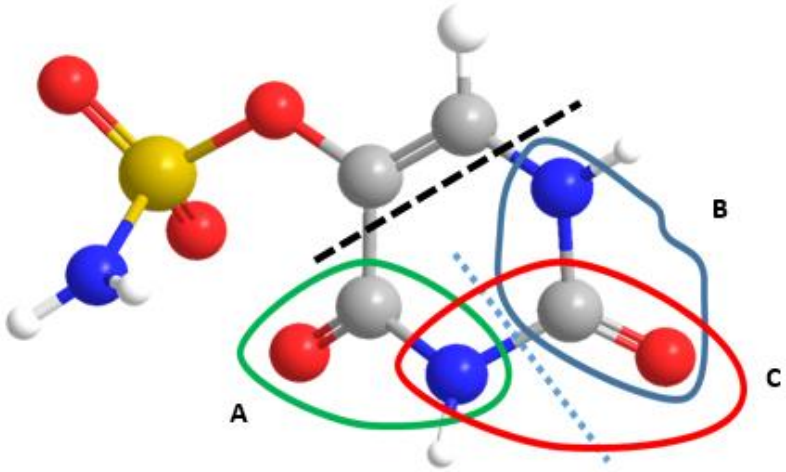

Figure S4. Possible channels leading to the formation of the OCN^- anion. The formation of OCN^- at m/z 42 can occur via any of the three possible channels as represented in the figure. The most probable channels for OCN^- formation are **A** (marked in green) and **B** (marked in blue), respectively, which occurs via multiple bond cleavages, i.e. N–C bond and C–C bond cleavage (black dots). A subsequent C–N bond scission (marked blue dots) and the loss of 2–H atoms leads to the formation either channels A and/or B. The channel C (marked in red) is as well possible but with different bond cleavages.

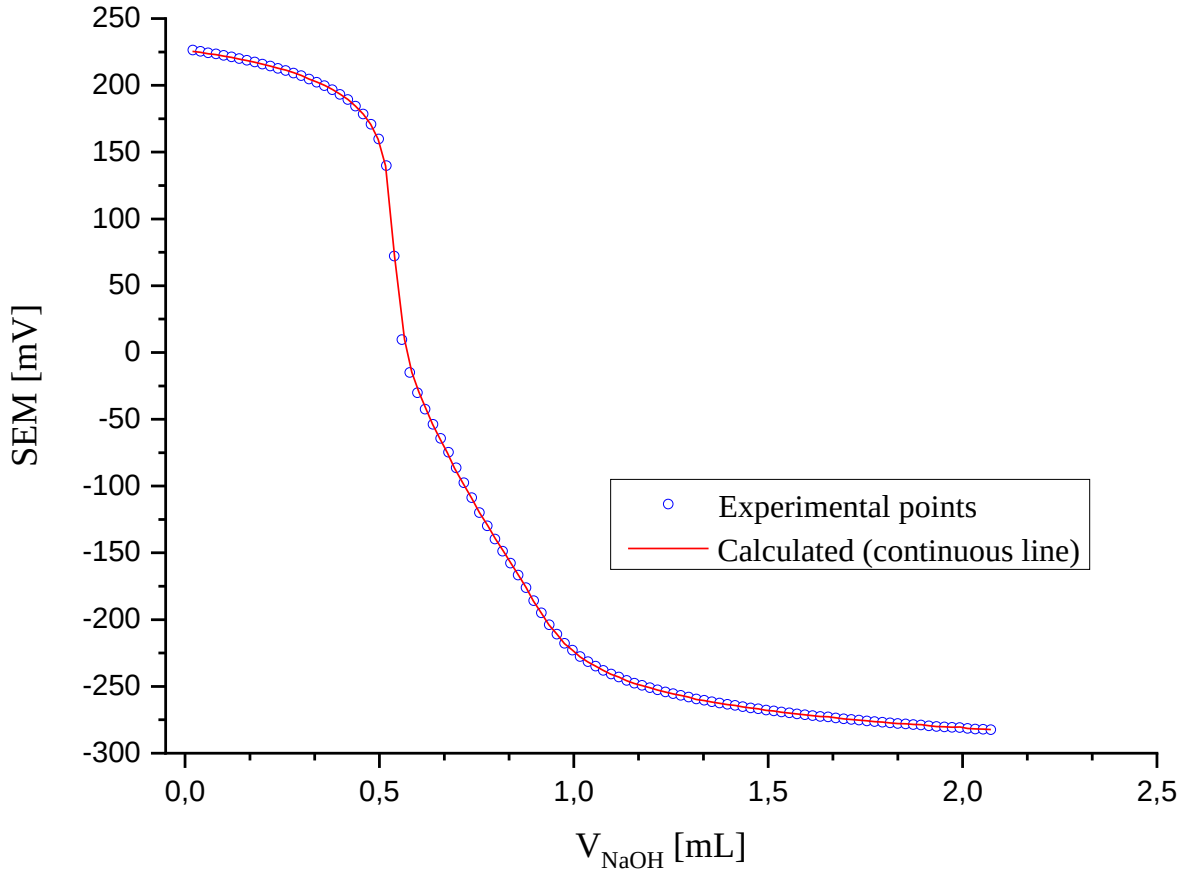

Figure S5. The representative titration curve: SEM = *f*(V_{NaOH}) of the 1 mM uracil-5-yl *O*-sulfamate and 2.55 mM HCl solution (the initial volume 5.0 mL) titrated with the standardized 24 mM NaOH solution at 298.15 K.

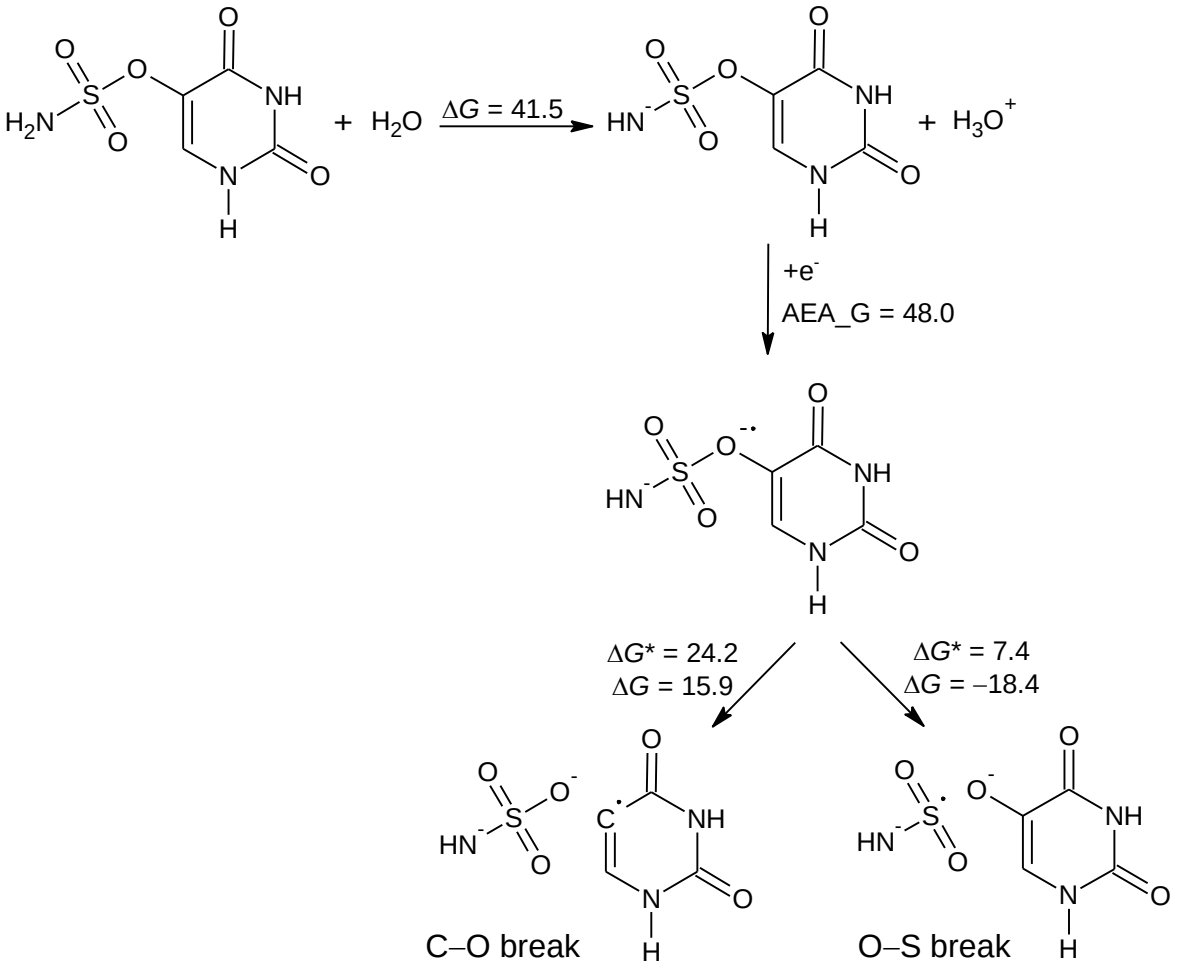

Scheme S1. Dissociative electron attachment process calculated for deprotonated anionic form of uracil-5-yl *O*-sulfamate at M06-2X/6-31++G(d,p) level, PCM water solution. AEA_G refers to adiabatic electron affinity (Gibbs free energy scale), while Δ*G* and Δ*G** refer to thermodynamic and kinetic barriers (Gibbs free energy scale, too). All presented values are given in kcal/mol.

Possible electron-induced degradation paths for the deprotonated anionic forms of SU have been calculated at the DFT level (M06-2X/6-31++G(d,p), PCM water solution). It is worth emphasizing that the minor role of deprotonation process has been proved in radiolysis experiments at various pHs (4 < pH < 8). Indeed, regardless of pH SU does not decompose. The above mentioned experimental results are compatible with the DFT calculations for deprotonated anionic SU DEA degradation – see Scheme S1. First of all, electron attachment to the anionic SU (leading to the radical dianion) is less favorable than electron attachment to the neutral SU form (leading to anion radical SU) – the adiabatic electron affinity (AEA) calculated for deprotonated anionic SU is substantially lower than AEA calculated for neutral SU (48 vs. 61 kcal/mol). The following steps, namely breaking the C–O or O–S bonds in the dianion radical SU (see Scheme S1), are less probable than in the case of anion radical SU, too. Breaking the C–O bond is unfavorable even thermodynamically (Δ*G* = 15.9 kcal/mol, see

Scheme S1). On the other hand, breaking the O–S bond could seem to be probable, with its relatively low activation barrier (ΔG^* = 7.4 kcal/mol) and favorable thermodynamic stimulus (ΔG = −18.4 kcal/mol). However, one should bear in mind that the kinetic barrier for O–S break in the anion radical is as low as 2.3 kcal/mol and the thermodynamic stimulus for this process as large as −39.4 kcal/mol (all the data were calculated at the M06-2X level) and no evidence of O–S bond break was found in the radiolytic experiment. Thus, the underestimated M06-2X barrier for the O–S bond scission probably leads to a suggestion that the S–O bond dissociation may take place in the sulfamate dianion.

Complete References:

(50) Frisch, M. J.; Trucks G. W.; Schlegel, H. B.; Scuseria, G. E.; Robb, M. A.; Cheeseman, J. R.; Scalmani, G.; Barone, V.; Petersson, G. A.; Nakatsuji, H.; L,i X.; Caricato, M.; Marenich, A. V.; Bloino J.; Janesko, B. G.; Gomperts, R.; Mennucci, B.; Hratchian, H. P.; Ortiz, J. V.; Izmaylov, A. F.; Sonnenberg, J. L.; Williams-Young, D.; Ding, F.; Lipparini, F.; Egidi, F.; Goings, J.; Peng, B.; Petrone, A.; Henderson, T.; Ranasinghe, D.; Zakrzewski, V. G.; Gao, J.; Rega, N.; Zheng, G.; Liang, W.; Hada, M.; Ehara, M.; Toyota, K.; Fukuda, R.; Hasegawa, J.; Ishida, M.; Nakajima, T.; Honda, Y.; Kitao, O.; Nakai, H.; Vreven, T.; Throssell, K.; Montgomery, J. A., Jr.; Peralta, J. E.; Ogliaro, F.; Bearpark, M. J.; Heyd, J. J.; Brothers, E. N.; Kudin, K. N.; Staroverov, V. N.; Keith, T. A.; Kobayashi, R.; Normand, J.; Raghavachari, K.; Rendell, A. P.; Burant, J. C.; Iyengar, S. S.; Tomasi, J.; Cossi, M.; Millam, J. M.; Klene, M.; Adamo, C.; Cammi, R.; Ochterski, J. W.; Martin, R. L.; Morokuma, K.; Farkas, O.; Foresman, J. B.; Fox, D. J. *Gaussian 16*, Revision C.01, Gaussian, Inc.: Wallingford, CT, 2019.

(51) Frisch, M. J.; Trucks, G. W.; Schlegel, H. B.; Scuseria, G. E.; Robb, M. A.; Cheeseman, J. R.; Scalmani, G.; Barone, V.; Mennucci, B.; Petersson, G. A.; Nakatsuji, H.; Caricato, M.; Li, X.; Hratchian, H. P.; Izmaylov, A. F.; Bloino, J.; Zheng, G.; Sonnenberg, J. L.; Hada, M.; Ehara, M.; Toyota, K.; Fukuda, R.; Hasegawa, J.; Ishida, M.; Nakajima, T.; Honda, Y.; Kitao, O.; Nakai, H.; Vreven, T.; Montgomery, J. A., Jr.; Peralta, J. E.; Ogliaro, F.; Bearpark, M. J.; Heyd, J.; Brothers, E. N.; Kudin, K. N.; Staroverov, V. N.; Kobayashi, R.; Normand, J.; Raghavachari, K.; Rendell, A. P.; Burant, J. C.; Iyengar, S. S.; Tomasi, J.; Cossi, M.; Rega, N.; Millam, N. J.; Klene, M.; Knox, J. E.; Cross, J. B.; Bakken, V.; Adamo, C.; Jaramillo, J.; Gomperts, R.; Stratmann, R. E.; Yazyev, O.; Austin, A. J.; Cammi, R.; Pomelli, C.; Ochterski, J. W.; Martin, R. L.; Morokuma, K.; Zakrzewski, V. G.; Voth, G. A.; Salvador, P.; Dannenberg, J. J.; Dapprich, S.; Daniels, A. D.; Farkas, Ö.; Foresman, J. B.; Ortiz, J. V.; Cioslowski, J.; Fox, D. J. *Gaussian 09*, Revision D.01; Gaussian, Inc.: Wallingford, CT, 2013.